Transgenic Models to Study Gonadotropin Function: The Role of Follicle-Stimulating Hormone in Gonadal Growth and Tumorigenesis

T. Rajendra Kumar, Ganesh Palapattu, Pei Wang, Teresa K. Woodruff, Irving Boime, Michael C. Byrne, and Martin M. Matzuk

Department of Pathology (T.R.K., G.P., P.W., M.M.M)
Department of Cell Biology (M.M.M.)
Department of Molecular and Human Genetics (M.M.M.)
Baylor College of Medicine
Houston, Texas 77030

Department of Medicine and Neurobiology and Physiology (T.K.W.)
Northwestern University
Chicago, Illinois 60611

Department of Molecular Biology and Pharmacology (I.B.)
Washington University School of Medicine
St. Louis, Missouri 63110

Genetics Institute (M.C.B.)
Cambridge, Massachusetts 02140

The role of FSH in gonadal tumorigenesis and, in particular, in human ovarian cancer has been debated. It is also unclear what role the elevated FSH levels in the inhibin-deficient mouse play in the gonadal tumorigenesis. To directly assess the role of FSH in gonadal growth, differentiation, and gonadal tumorigenesis, we have generated both gain-of-function and loss-of-function transgenic mutant mice. In the gain-of-function model, we have generated transgenic mice that ectopically overexpress human FSH from multiple tissues using a mouse metallothionein-1 promoter, achieving levels far exceeding those seen in postmenopausal women. Male transgenic mice are infertile despite normal testicular development and demonstrate enlarged seminal vesicles secondary to elevated serum testosterone levels. Female transgenic mice develop highly hemorrhagic and cystic ovaries, have elevated serum estradiol and progesterone levels, and are infertile, mimicking the features of human ovarian hyperstimulation and polycystic ovarian syndromes. Furthermore, the female transgenic mice develop enlarged and cystic kidneys and die between 6–13 weeks as a result of urinary bladder obstruction. In a complementary loss-of-function approach, we have generated double-homozygous mutant mice that lack both inhibin and FSH by a genetic intercross. In contrast to male mice lacking inhibin alone, 95% of which die of a cancer cachexia-like syndrome by 12 weeks of age, only 30% of the double-mutant male mice lacking both FSH and inhibin die by 1 yr of age. The remaining double-mutant male mice develop slow-growing and less hemorrhagic testicular tumors, which are noted after 12 weeks of age, and have minimal cachexia. Similarly, the double-mutant female mice develop slow-growing, less hemorrhagic ovarian tumors, and 70% of these mice live beyond 17 weeks. The double-mutant mice demonstrate minimal cachexia in contrast to female mice lacking only inhibin, which develop highly hemorrhagic ovarian tumors, leading to cachexia and death by 17 weeks of age in 95% of the cases. The milder cachexia-like symptoms of the inhibin and FSH double-mutant mice are correlated with low levels of serum estradiol and activin A and reduced levels of aromatase mRNA in the gonadal tumors. Based on these and our previous genetic analyses, we conclude that elevated FSH levels do not directly cause gonadal tumors. However, these results suggest FSH is an important trophic modifier factor for gonadal tumorigenesis in inhibin-deficient mice. (Molecular Endocrinology 13: 851–865, 1999)

0888-8809/99/$3.00/0
Molecular Endocrinology

INTRODUCTION

Members of the pituitary and placental glycoprotein hormone family are heterodimers, which share a common α-subunit that is noncovalently linked to a hormone-specific β-subunit (1). The pituitary gonadotropins LH and FSH bind to structurally related but distinct receptors in the gonads and control gonadal growth, differentiation, and steroidogenesis. FSH receptors (FSHRs) are localized to Sertoli cells in the testis and granulosa cells in the ovary (2). Expression of the glycoprotein α-subunit and the hormone-specific FSHβ-subunit is regulated by the hypothalamic peptide GnRH, steroids, and the gonadal and pituitary peptides, activins, and inhibins (3, 4).

To generate animal models for human diseases involving the gonadotropin signal transduction pathway, we recently produced loss-of-function mice deficient in the FSHβ-subunit using embryonic stem cell technology (5). FSH-deficient female mice are infertile and demonstrate small ovaries resulting from a block in folliculogenesis at the preantral stage. In contrast, male mice deficient in FSH are fertile despite having small testes with reduced sperm number and motility (5). This loss-of-function model phenocopies human primary amenorrhea due to defective FSHR signaling in the ovary (6). Although loss-of-function mutations in the FSHβ gene or FSHR gene could explain some forms of female infertility, including ovarian dysgenesis and hypogonadism, it is unclear whether ovarian hyperstimulation syndromes and ovarian cancer in women are due to elevated FSH levels or altered FSH signaling in the ovary.

Inhibins are members of the transforming growth factor-β superfamily that includes important proteins such as activins, growth differentiation factor-9, and Müllerian-inhibiting substance (7). Inhibins were originally discovered as gonadal peptides that suppress pituitary FSH synthesis and secretion (8). The major sites of inhibin production in the gonads are Sertoli cells in the testis and granulosa cells in the ovary (9). To study gonadal growth and differentiation, we earlier generated an animal model in which mice deficient in inhibin develop multiple sex cord-stromal tumors (*i.e.* granulosa/Sertoli cell tumors) as early as 4 weeks of age with 100% penetrance (10). These tumors are usually multifocal and often hemorrhagic and secrete large amounts of estradiol and activins into circulation (4). The gonadal tumor-prone inhibin-deficient mice display characteristic hunchback and sunken eye appearance and eventually die as a result of a severe wasting (cancer cachexia-like) syndrome accompanied by hepatocellular necrosis around the central vein and a block in differentiation of several gastric cell lineages (11). Thus, inhibin was identified as a novel secreted tumor suppressor with gonadal specificity. Consistent with the known role of inhibin to negatively regulate FSH, inhibin-deficient mice demonstrate elevated levels of serum FSH. Although these types of gonadal tumors are rare in humans, elevated levels of serum FSH have been associated with some forms of ovarian epithelial cancers in elderly women (12). However, to date, there is no direct *in vivo* evidence to support the involvement of elevated levels of FSH in gonadal tumorigenesis. Earlier we showed that mice deficient in inhibin and GnRH (and therefore have suppressed levels of FSH and LH) survive for more than 1 yr and do not develop cachexia. These mutant male mice do not develop testicular cancers, but females show only premalignant lesions in the ovary (13). Although these studies indicated that gonadotropins (FSH and LH) are essential modifier factors for gonadal sex cord-stromal tumor development, we could not delineate the individual roles of FSH and LH in this pathway.

In this manuscript, we have addressed the biological role of FSH in gonadal growth and tumorigenesis. Using genetic approaches, including the production of gain-of-function transgenic mice overexpressing human FSH (hFSH) [expressed from a mouse metallothionein-1 (mMT-1) promoter], we have studied gonadal development. In an independent set of experiments, using a loss-of-function approach and genetic intercrosses, we generated double-homozygous mutant mice that are deficient in both inhibin and FSH to examine the role of FSH in gonadal tumor development/progression in these mice.

RESULTS

Generation of MT-α and MT-hFSHβ Transgenic Mice and Analysis of Fertility

To produce mice overexpressing hFSH, we initially generated, via pronuclear microinjection, transgenic mice carrying either MT-α or MT-hFSHβ transgenes. Using an hCGα-specific probe fragment, we identified two MT-α male founder mice that had approximately 50–60 copies of the MT-α transgene. The 700-bp human α-probe fragment, which did not hybridize to the endogenous mouse-α subunit gene sequences, permitted us to unequivocally identify the MT-α transgene-positive mice. In an independent set of pronuclear microinjection experiments, four MT-hFSHβ founder mice (two male and two female) were identified using an hFSHβ-specific 3′-untranslated region (UTR) probe. Southern blot analysis and breeding experiments confirmed that one male founder (line 2) had less than 5 copies of the transgene, and the other (line 1) had 2 chromosomal integrations of the hFSHβ transgene (see below). At one site, less than 5 copies of the transgene had integrated, and at the other site, approximately 50 copies were independently segregated and were transmitted to progeny successfully. Both of the female founder mice had approximately 50 copies of the transgene.

To determine the tissue sites of expression of the transgenes, we prepared total RNA from different tissues of the hFSH transgenic mice, and duplicate RNA blots were separately hybridized with either an hCGα probe or an hFSHβ 3′-UTR probe and subsequently stripped and reprobed with an 18S rRNA probe. As shown in Fig. 1, both of the transgenes (hCGα in Fig. 1A and hFSHβ in Fig. 1B) are expressed in multiple tissues with the highest level of expression in the liver.

Both of the MT-α founders were fertile and stably transmitted the transgene to subsequent generations. Similarly, the low copy-bearing MT-hFSHβ male founders, the female progeny derived from these lines, and one male founder bearing high-copy MT-hFSHβ transgene were all fertile. These mice stably transmitted the transgene for several subsequent generations. In sharp contrast, both female founders that contained 50 copies of the MT-hFSHβ transgene were infertile and never mated to proven fertile male mice over a 6-month period. Histological analyses performed on the ovaries from these founders and female progeny mice obtained from the high-copy male founder confirmed that these mice did not undergo estrous cycles. In contrast to ovaries from control female mice (Fig. 2E), there were no obvious corpora lutea, and many of the sections obtained from these ovaries showed accumulation of a periodic acid Schiff (PAS)-positive substance in the interstitial cells (Fig. 2F). Immunohistochemical analysis using a hFSHβ-specific monoclonal antibody confirmed that the PAS-positive material in the interstitial cells was hFSHβ (data not shown). In ovaries from many of the older female transgenic mice containing multiple copies of the hFSHβ transgene, there were often visible fluid-filled cysts, and morphologically the ovaries looked pale yellow in contrast to the highly vascularized ovaries in wild-type littermate mice. There were no obvious defects in oocytes or granulosa and thecal cells. Thus, the high-copy hFSHβ transgene carrying female mice demonstrate intraovarian defects of unknown etiology leading to infertility. It is unclear whether the high levels of free FSHβ subunit in the ovarian interstitial cells are interfering with some key function.

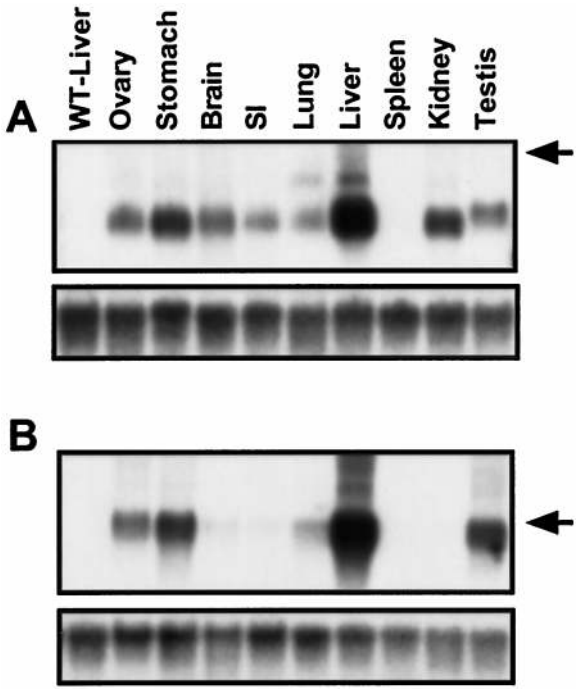

Fig. 1. Northern Blot Analysis of Transgene Expression in Adult Tissues

Total RNA (15 μg) extracted from various tissues of adult transgenic mice was subjected to Northern blot hybridization. Total RNA from a wild-type (WT) mouse liver was used as a negative control. One blot was probed with 700 bp of *Hin*dIII-*Hin*dIII (exon-2) hCGα-specific sequences (*top panel in A*). The other blot was probed with 450 bp of *Pst*I-*Bam*HI (3′-UTR) hFSHβ-specific sequences (*top panel in B*). Note the expression of transgenes in multiple tissues. Equivalent loading of RNA was confirmed by hybridization with a ribosomal 18S cDNA probe (*bottom panels in A and B*). The *arrows* indicate the relative migration positions of the 18S rRNA on the blots.

Generation of hFSH Transgenic Mice and Analysis of Serum Levels of hFSH and Steroids

FSH biological activity requires heterodimerization of the individual subunits. To obtain hFSH-overexpressing mice, we intercrossed the MT-α and MT-hFSHβ lines of mice. The progeny mice were screened by Southern blot analysis, and mice positive for both transgenes were identified. Reciprocal crosses were made between both sexes of MT-α and low-copy MT-hFSHβ mice. This line of mice is referred to as weak hFSH expressors. Both male and female weak hFSH (*i.e.* dimer) expressors were fertile and indistinguishable from the control wild-type littermates. These mice did not show any gross phenotypic abnormalities or any pathology upon detailed surgical and histological analysis when analyzed up to 1 yr of age. The description and use of the weak hFSH expressors (*i.e.* 48.0 and 115.9 mIU/ml hFSH for males and females, respectively) have been published previously (14).

Since high-copy MT-hFSHβ females were infertile, male mice with the high-copy number hFSHβ transgene were bred to female mice that carry the MT-α transgene. The resulting mice that carry both transgenes are referred to as high-copy hFSH (dimer) expressors. All further analyses described in this manuscript were carried out on the high-copy hFSH expressors, and hereafter these mice will be referred to as hFSH (*i.e.* dimer) transgenic mice.

To determine the level of expression of the transgene mRNA driven by the mMT-1 promoter under basal conditions, we analyzed the levels of hFSH in the mouse serum using a specific fluoroimmunoassay that did not cross-react with endogenous mouse FSH and did not detect the hFSHβ subunit. In addition, we

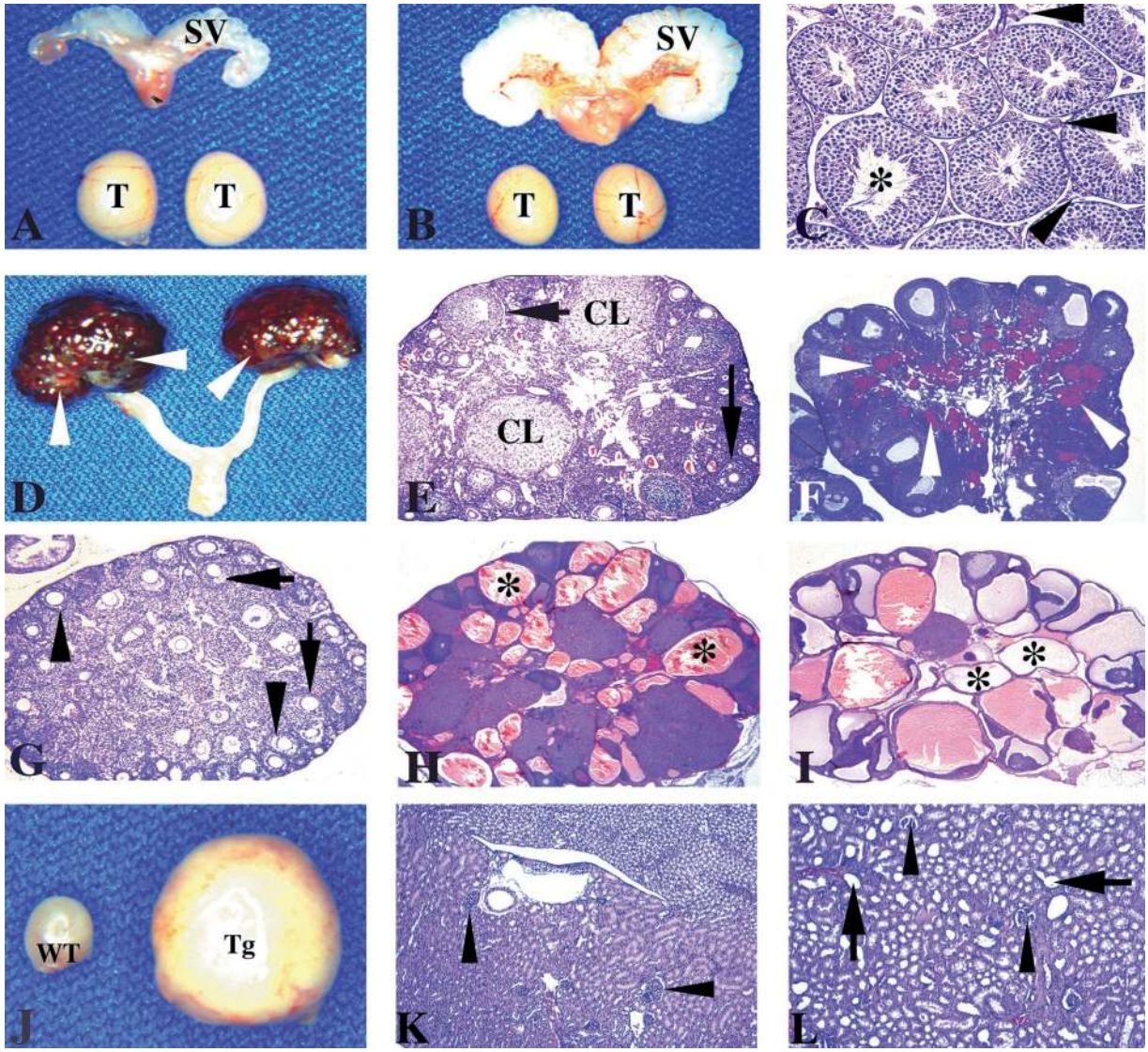

Fig. 2. Morphological and Histological Analysis of Wild-Type and MT-FSH Transgenic Male (A–C) and Female (D–L) Mice

A and B, Gross analysis of the testis (T) and seminal vesicles (SV) from 5-week-old littermate wild-type (A) and transgenic (B) male mice. Note the normal size of the testis and enlarged seminal vesicles in panel B compared with panel A. Although the male transgenic mice are infertile, histological analysis of the testis (C) from a 7-week-old male transgenic mouse shows normal Leydig cells (*arrowheads*) and many late-stage spermatids. The abundant sperm tails in the lumen are indicated with an *asterisk* in panel C. D, Gross analysis of the ovary and uterus from a 6-week-old female transgenic mouse. Note the presence of many hemorrhagic cysts (*white arrowheads*) in the enlarged ovaries. Histological analysis of an ovary from a 9-week-old wild-type female mouse (E) shows follicles in multiple stages; secondary (*long arrow*) and early antral stage follicle (*short arrow*) are indicated. Corpora lutea (CL) are clearly seen. Ovarian histology of an 8-month-old infertile female mouse expressing only the hFSHβ subunit (F) demonstrates PAS-stained material (*white arrows*) in many interstitial cells between the follicles. Note the absence of late-stage follicles and corpora lutea. Histology of an ovary from a 2-week-old MT-hFSH transgenic female mouse (G) shows normal initiation of folliculogenesis (*black arrow*, *black arrowhead*) but by 6 weeks (H) or 7 weeks (I), massive hemorrhagic cysts and fluid-filled cysts are noticeable (*asterisks*). Panel G was photographed at low power and panels H and I were photographed at medium power. J–L, Urinary tract abnormalities in MT-hFSH transgenic female mice. J, Gross analysis of urinary bladder from 7-week-old wild-type (WT) and hFSH transgenic (Tg) female mice. Note the enlarged urinary bladder from the transgenic mice caused by deposition of hFSH-like immunoreactive material. Comparison of kidney histology from 8-week-old wild-type (K) and transgenic (L) female mice. *Arrowheads* point to the glomeruli. Note the many enlarged tubules (*arrows*) in the transgenic kidney (L). Panels K and L were photographed at the same magnification.

measured the steroid hormone levels by specific RIAs. Both of these studies demonstrated high levels of these hormones in adult transgenic mice compared with age-matched wild-type littermates (Table 1 and see below). These results confirm that the hFSH heterodimer could be efficiently assembled, processed,

Table 1. Serum Levels of hFSH, Estradiol, Progesterone, Testosterone, and IGF-1 in Female Mice[a]

Genotype	hFSH[b] (mIU/ml)	Estradiol[c] (pg/ml)	Progesterone[d] (ng/ml)	Testosterone[e] (ng/ml)	IGF-1[f] (ng/ml)	LH[g] (ng/ml)
Wild-type	0	<5	6.2 ± 0.2*	<0.1	633.3 ± 23.0	7.3 ± 3.0
MT-hFSH	362,000 ± 5,500	194.6 ± 26.5	150 ± 20.9†	5.9 ± 0.7	627.3 ± 51.4	7.9 ± 2.2

[a] Randomly cycling adult female mice (6–9 weeks of age) were used; values are mean ± SEM, n = 6–10.
[b] Estimated by a fluoroimmunoassay; sensitivity = 0.3 mIU/ml.
[c] Estimated by an ultrasensitive liquid phase double-antibody RIA; sensitivity = 5 pg/ml.
[d] Estimated by a solid phase RIA; sensitivity = 0.3 ng/ml; * *vs.* †, $P < 0.05$.
[e] Estimated by a solid phase RIA; sensitivity = 0.1 ng/ml.
[f] Estimated by an acid-ethanol extraction method using a rat IGF-1 RIA kit.
[g] Estimated by a rat LH RIA (NIDDK); sensitivity = 5 ng/ml.

and secreted in large quantities from multiple tissues of these transgenic mice. In addition, these data also suggest that this ectopically produced hFSH is biologically active, leading to enhanced gonadal steroid output into the serum.

hFSH Transgenic Male Mice Are Infertile and Have Enlarged Seminal Vesicles

To study the effects of high serum levels of hFSH (151,000 ± 2,400 mIU/ml, n = 7) on male fertility, adult transgenic male mice (6–8 weeks) were mated to wild-type randomly cycling females. Nine of 10 males were infertile over 6 months. The one male that successfully mated with a female did it once over this 6-month period, with one litter delivered, but this male subsequently was infertile. In a separate experiment, 4 of 4 MT-hFSH transgenic males failed to mate (no visible vaginal plugs) to PMSG/hCG-primed immature wild-type female mice, confirming that these male mice were infertile. To determine the causes of the infertility, morphological and histological analyses of the gonads from these mice were performed at different time points. There were no statistical differences in testicular size (mean ± SEM) examined at 6 weeks of age (90.0 ± 1.6 mg for transgenic *vs.* 90.8 ± 2.9 mg for wild-type, n = 8; $P > 0.05$) or at earlier time points (data not shown), and the testes from transgenic mice appeared morphologically indistinguishable from those of the wild-type control mice (Fig. 2, A and B). Likewise, there were no differences in the weights of the epididymides. However, the seminal vesicles from the transgenic mice were enlarged, appeared highly translucent, and were greater than 2-fold larger (Fig. 2B) compared with the age-matched wild-type male mice (Fig. 2A; 223.1 ± 10.9 mg, transgenic *vs.* 105.3 ± 10.2 mg, wild-type, n = 6; $P < 0.05$). The seminal vesicles were enlarged as early as 3 weeks of age in the male transgenic mice consistent with elevated testosterone levels in the serum (36.8 ± 6.7 ng/ml, transgenic *vs.* 1.9 ± 1.5 ng/ml, wild-type, n = 5; $P < 0.05$). In addition, histological analysis of the testes did not show any obvious defects. The tubules appeared healthy and intact and contained abundant spermatoza in the lumen, and normal numbers of Leydig cells were observed in the interstitial spaces (Fig. 2C). To examine whether there were any quantitative differences in sperm parameters, epididymal sperm from 6-week-old wild-type and transgenic male mice were analyzed. There was a significant increase in sperm number in the transgenic male mice ($1.4 \pm 0.2 \times 10^7$, transgenic *vs.* $0.8 \pm 0.1 \times 10^7$, wild-type, n = 5; $P < 0.05$), but no significant differences were observed in motility or viability when wild-type and transgenic mice were compared (data not shown). Castration of 42-day-old male transgenic mice resulted in regression of the seminal vesicles similar to castrated age-matched wild-type male mice (23.9 ± 5.9 mg, transgenic *vs.* 19.4 ± 1.8 mg, wild-type, n = 6; $P > 0.05$). This experiment suggested that the increased size of the seminal vesicle was due to the elevated testosterone and not a direct action of the hFSH on the seminal vesicles. Thus, these hFSH-expressing male mice are essentially infertile, demonstrate high levels of serum testosterone, and have enlarged seminal vesicles. Based on our experiments, the infertility in these hFSH-expressing transgenic male mice could be due to some reproductive behavioral defects because of either the high hFSH or the high testosterone levels in the serum.

hFSH-Overexpressing Female Mice Are Infertile and Develop Hemorrhagic and Cystic Ovaries

More than 95% of the female transgenic mice appeared weak and died between 6–9 weeks. To study the gain-of-function effects of hFSH in female mice, reproductive tracts were examined morphologically and histologically. At 6 weeks of age, ovaries from the transgenic female mice were completely hemorrhagic and enlarged and appeared cystic (Fig. 2D). The uteri were fluid filled and enlarged and appeared translucent (Fig. 2D). These phenotypic characteristics were obvious as early as 2 weeks of age. In contrast to control female mice (Fig. 2E), histological analysis of the ovaries of these adult hFSH-transgenic female mice demonstrated minimally intact follicular architecture and no progression of follicles beyond the preantral follicle stage with massive hemorrhagic and cystic islands within the ovaries (Fig. 2, H and I). However, those follicles that remained intact

showed normal-appearing oocytes and granulosa and thecal layers. The ovarian defects and hemorrhage appeared less severe at earlier time points, and histological analysis showed the initiation of hemorrhage and cyst formation as discrete foci. Furthermore, as early as 2 weeks, the ovarian histology appeared normal with many immature follicles including primary and early antral follicles (Fig. 2G). In two of the female transgenic mice that survived to 13 weeks of age, the ovaries were massively hemorrhagic and cystic with no apparent signs of folliculogenesis. In addition, there were no obvious signs of any tumors (data not shown). Consistent with these morphological and histological findings, all of the female transgenic mice were infertile. Serum IGF-I and LH levels, which are known to be elevated in human polycystic ovarian disease, did not show any differences between wild-type and hFSH-overexpressing female mice (Table 1). There were no apparent defects in other tissues examined except for the kidneys and bladders (described below). These findings in the hFSH-overexpressing female mice resemble some of the features of gonadotropin-induced ovarian hyperstimulation in human patients (see *Discussion*).

Urinary Tract Abnormalities in hFSH-Overexpressing Female Mice

The immediately obvious defects secondary to excessive stimulation of the ovaries were enlarged kidneys and urinary bladders in the majority of the hFSH-transgenic female mice. Morphologically, the bladders of the transgenic mice appeared thick and filled with deposition of a white proteinaceous stone-like material (Fig. 2J). Although the bladder enlargement was apparent as early as 3–4 weeks, only mice that were more than 6 weeks old demonstrated this accumulation inside the bladder. This material could be extracted into 0.1 N HCl and was found to be immunoreactive in an FSH RIA (data not shown). As the deposition of this immunoreactive FSH-like material progressed in the bladder, the urinary output declined, and in two 13-week-old mice, there was no obvious sign of urine in the bladder. Consistent with these observations, the kidneys were enlarged and sometimes even cystic. Histological analysis of the kidneys from these animals demonstrated that the architecture of many of the glomeruli was damaged (Fig. 2L), the tubules were enlarged, and there was a significant infiltration of macrophage-like cells at different sites within the tubules (not shown). These results suggest that the majority of the hFSH-overexpressing female mice developed urinary tract obstruction leading to death.

The Majority of the $inha^{m1}/inha^{m1}$, $fshb^{m1}/fshb^{m1}$ Double-Homozygous Mutant Mice Fail to Develop a Wasting Syndrome

To determine the role of FSH in gonadal tumor development, we generated double-homozygous mutant mice that lack both inhibin and FSH by a genetic cross. The first overt sign of gonadal tumor development in inhibin-deficient mice is severe weight loss caused by an activin-related cachexia-like syndrome that eventually results in the death of these mice (11). Therefore, the double-homozygous mutant mice were weighed weekly, the weights were compared with those of mice deficient only in inhibin ($inha^{m1}/inha^{m1}$), and the percentage of survivors was calculated. As seen in Fig. 3A, 95% of the inhibin-deficient male mice die by 12 weeks of age. In sharp contrast, the majority of the double-homozygous mutant male mice survived to 1 yr and did not show any dramatic weight loss. Alternatively, about 70% of the female double-homozygous mutant mice survived past 17 weeks. However, 100% of them eventually lost weight and died by 39 weeks, in contrast to 95% of the female mice deficient in inhibin alone that die by 17 weeks (Fig. 3B). These results suggest that absence of FSH was affecting the gonadal tumor development/progression in inhibin-deficient mice.

Altered Gonadal Tumor Development/Progression in $inha^{m1}/inha^{m1}$, $fshb^{m1}/fshb^{m1}$ Double-Homozygous Mutant Mice

The bilateral tumors in inhibin-deficient male mice were evident as early as 4 weeks of age. Initially, small foci of nodular proliferation appeared upon histological examination. These foci progressed very rapidly and finally became focally hemorrhagic and invasive (Fig. 4, A and B). Similarly, 9- to 12-week-old female mice deficient in inhibin demonstrated hemorrhage and disruption of the normal follicular architecture of the invasive tumors. These tumors often contained masses of granulosa cells, undifferentiated gonadal stromal derivatives, or clusters of mitotically active stromal cells reminiscent of seminiferous tubules (*i.e.* mixed granulosa/Sertoli cell tumors) (Fig. 5D).

In contrast to $inha^{m1}/inha^{m1}$ mice, most of the $inha^{m1}/inha^{m1}$, $fshb^{m1}/fshb^{m1}$ double-mutant mice predominantly developed slow-growing gonadal tumors (Figs. 4C and 5B). These tumors, which initially appeared less hemorrhagic compared with the $inha^{m1}/inha^{m1}$ mice, were very small in a few of the 12-week-old double-mutant male mice (Fig. 4, C and D). Some of the double-homozygous mutant male mice (6 of 11) did not develop any tumors beyond 1 yr of age, and there were no signs of hemorrhage in the testes of these mice. Histological analysis performed on the testes from these double-mutant mice showed normal tubules that contained abundant sperm in the lumen and normal numbers of Leydig cells (Fig. 4, E and F). Testicular tumors that developed in some of the younger double-mutant male mice often failed to disrupt the gross tubular architecture; however, these tubules were often filled with proliferating tumor cells that appeared to be less aggressive (Fig. 4D), unlike those in the testes of $inha^{m1}/inha^{m1}$ male mice (10).

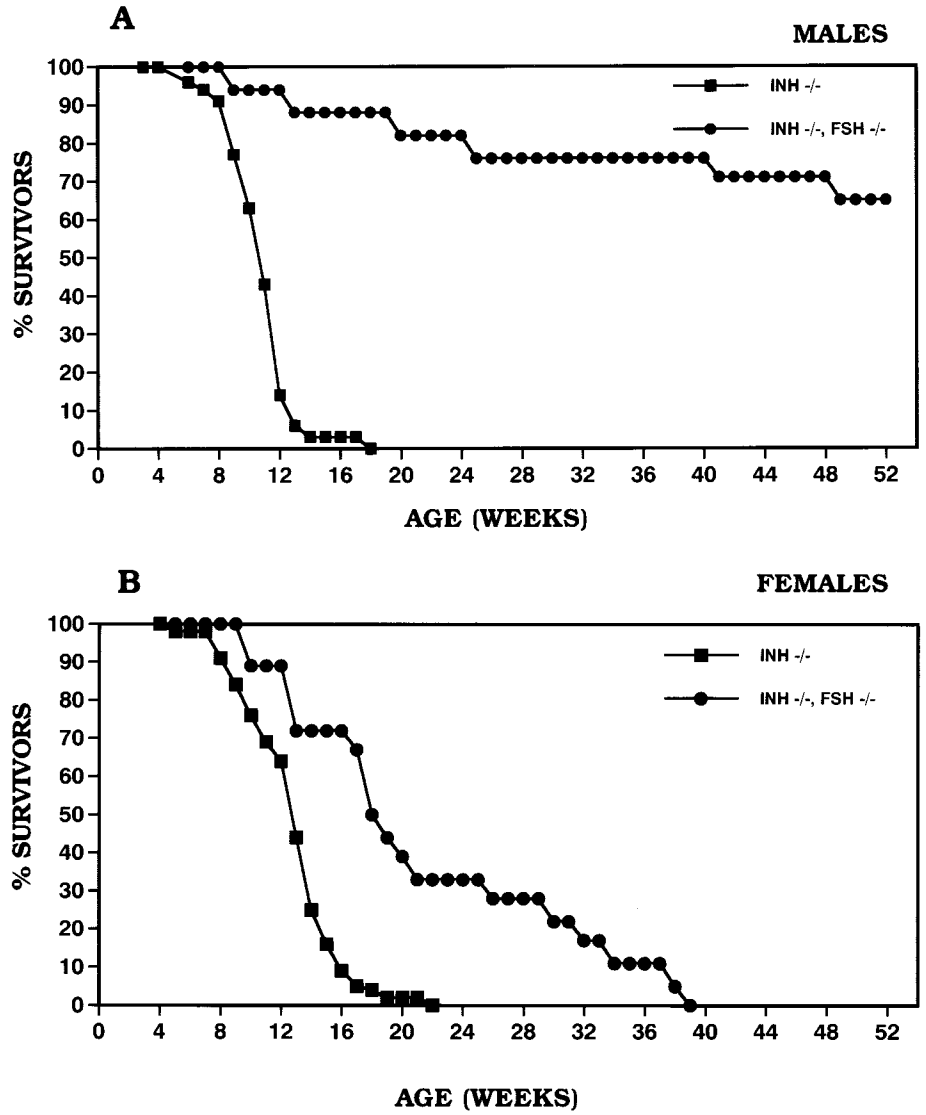

Fig. 3. Survival Curves for Inhibin-Deficient Mice and Double-Mutant Mice Deficient in Both Inhibin (INH) and FSH (FSH)

Each week, those mice that had not died or had not developed the severe wasting syndrome (and needed to be killed) were counted. In addition, body weights were recorded up to 1 yr. All mice were of the C57/129 mixed genetic background. The following numbers of mice were used: Inh −/−, 56 females and 38 males; Inh −/− and FSH −/−, 17 males and 18 females.

Thus, absence of FSH in the inhibin knockout male slows tumor development and, in some cases, prevents the formation of gonadal tumors.

Although at 12 weeks, the ovaries of some of the double-mutant female mice appeared normal morphologically (Fig. 5B), histological analysis on ovarian tumors obtained from double-homozygous mutant mice showed signs of hemorrhage and cyst formation as early as 12 weeks of age (Fig. 5G). At this and later stages, the ovaries contained obvious cysts with many tubule-like structures that resemble those in the ovaries of inhibin-deficient female mice (Fig. 5, E–H). Ovaries from some of the double-homozygous mutant female mice demonstrated bilateral mixed granulosa/Sertoli cell tumors that were less invasive (Fig. 5E). The spectrum of the histological features of these slow-growing and less invasive gonadal tumors in the double-homozygous mutant male and female mice is summarized in Table 2 and can be compared directly to mice lacking inhibin alone (10).

Functional Differences in Gonadal Tumors between $inha^{m1}/inha^{m1}$ and $inha^{m1}/inha^{m1}$, $fshb^{m1}/fshb^{m1}$ Double-Mutant Mice

Serum levels of activins become elevated as the gonadal tumors progress in inhibin-deficient mice, and the activin signaling through activin receptor type II causes liver and stomach defects (15). Since the ma-

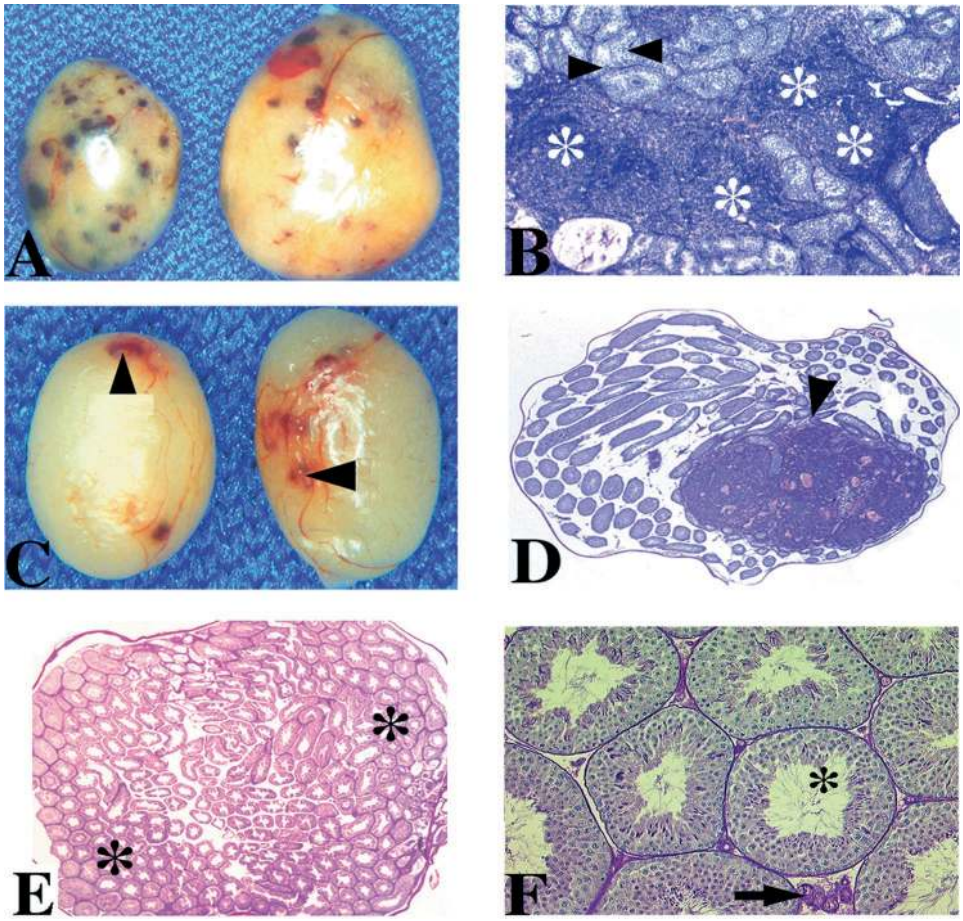

Fig. 4. Gross Analysis of the Testes of inha^{m1}/inha^{m1} (A) and inha^{m1}/inha^{m1}, fshb^{m1}/fshb^{m1} (C) Male Mice at 12 Weeks of Age

Note the multiple hemorrhagic spots and tumor in panel A compared with the small focal hemorrhagic areas (*arrowheads* in C) indicating delayed tumor growth in the absence of FSH. A section through the testicular tumor of a 12-week-old inha^{m1}/inha^{m1} male mouse (B) photographed at high power reveals multiple foci (*asterisks*) and obvious invasiveness of the expanding sex cord-stromal tumor. The tubules are indicated by *arrowheads*. In panel D, one focal tumor lesion filled with granulosa cells (*arrowhead*) is apparent whereas most of the tubular compartment remains intact in the testes of an inha^{m1}/inha^{m1}, fshb^{m1}/fshb^{m1} double-mutant male mouse at 12 weeks of age, photographed at lower magnification. E and F, Histological analysis of the testis of a 14-month-old fertile double-mutant male mouse showing normal tubules (*asterisks*). No signs of tumor foci are apparent in this low-power photomicrograph (E). A region of the same section at high-power magnification (F) shows several normal tubules. *Arrow* points to the Leydig cells. Tubules with many late-stage spermatozoa and abundant sperm tails in the lumen are clearly seen (*asterisk*).

jority of the double-homozygous mutant mice showed altered gonadal tumor development and no signs of cachexia, we examined functional differences, if any, when compared with mice deficient in inhibin only. Serum from male and female double-homozygous mutant mice that developed gonadal tumors was assayed for total activin A. The serum from these double mutants demonstrated significantly reduced levels of activin A compared with the serum from mice lacking inhibin alone (Table 3). Consistent with these results, the livers and glandular stomachs from these double-mutant mice did not show any morphological or histological abnormalities (data not shown). Whereas inhibin-deficient mice showed elevated levels of serum estradiol, serum levels were suppressed in the double-homozygous mutant mice (Table 3). In accordance with this, when total RNA prepared from inha^{m1}/inha^{m1} or inha^{m1}/inha^{m1}, fshb^{m1}/fshb^{m1} female mouse ovaries was hybridized with an aromatase probe, the levels were found to be significantly down-regulated in the double-homozygous mutant mice compared with inhibin-deficient mice (data not shown). Additionally, comparison of the large-scale gene expression profiles in the ovaries of wild-type and fshb^{m1}/fshb^{m1} female mice using an oligonucleotide-based gene chip assay revealed that activin βA and activin βB mRNAs were present in wild-type ovaries at 23 and 31 copies per million total copies of mRNA, respectively, but the mRNA for both subunits was undetectable in the knockout ovaries (M. C. Byrne, P. Wang, T. R. Kumar, and M. M. Matzuk, unpublished results). Furthermore, four of four double-homozygous mutant male mice up

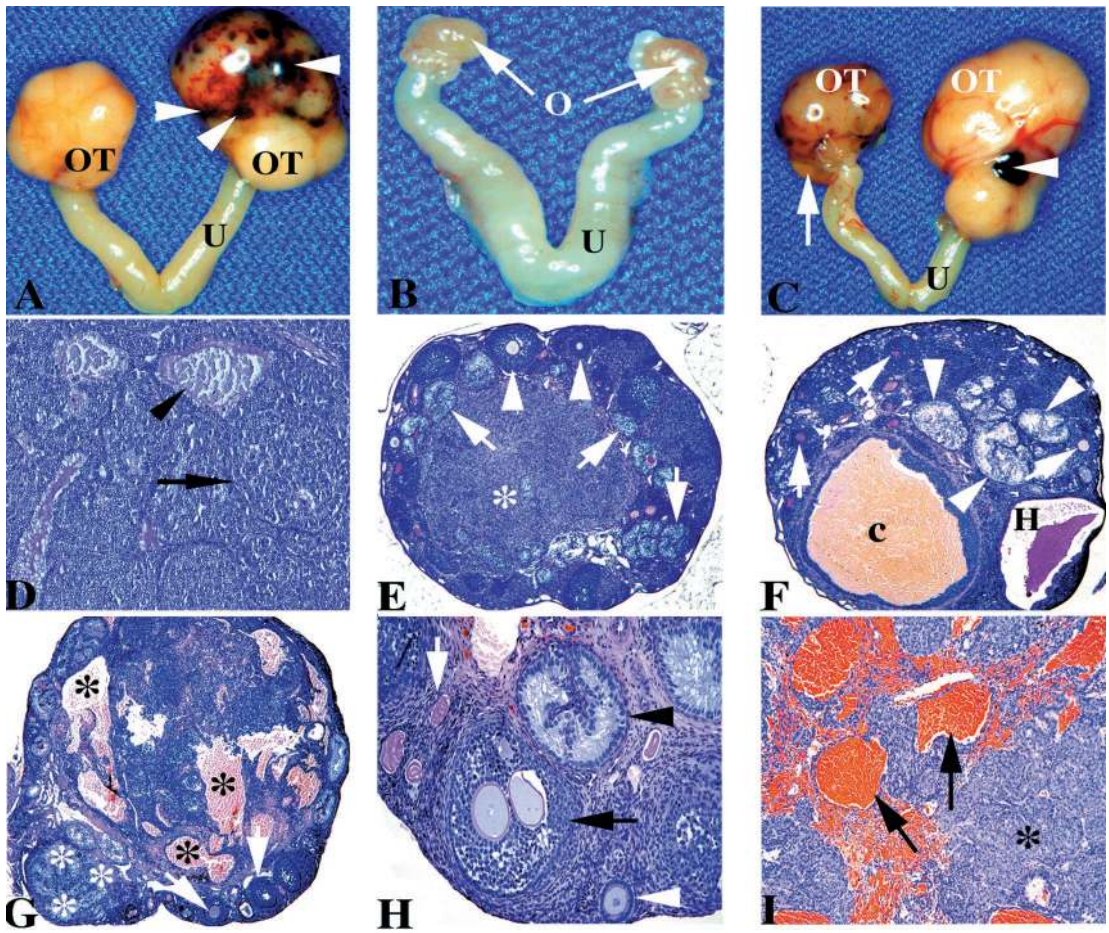

Fig. 5. Morphology and Histopathology of the Ovaries from inha^{m1}/inha^{m1} and inha^{m1}/inha^{m1}, fshb^{m1}/fshb^{m1} Female Mice

A–C, Gross analysis of the female reproductive tracts of inha^{m1}/inha^{m1} (A) and inha^{m1}/inha^{m1}, fshb^{m1}/fshb^{m1} double-mutant mice at 12 weeks (B) and 18 weeks (C), respectively. Whereas unilateral and/or bilateral hemorrhagic ovarian tumors are extremely large by 12 weeks in the absence of inhibin alone (A) by 12 weeks, at the same age, the ovaries from the majority of inhibin/FSH-deficient double-mutant female mice appear morphologically normal (B) without any signs of hemorrhage. However, ovarian tumors (OT) in some double-mutant female mice can be very large by 18 weeks (C). Note the similarity in ovarian tumor morphology in panel C compared with panel A. The hemorrhagic spots are indicated by *arrowheads* in panels A and C. *White arrow* in panel C points to a small cyst; U, uterus. D, Ovarian histology of a section of an 18-week-old inhibin-deficient female mouse showing aggressive proliferation of granulosa tumor cells. *Arrow* points to a tubule-like structure, and *arrowhead* points to an hemorrhagic spot. E–H, Histopathology of ovarian tumors obtained from inhibin/FSH-deficient double-mutant female mice of different ages. E, Low-power photograph of a 9-week-old double-mutant female mouse ovary contains normal follicles (*arrowheads*), many testicular tubule-like structures (*arrows*), and a slowly growing tumor in the center (*asterisk*). Hemorrhage and cysts are not apparent at this stage. F, At 12 weeks, an ovary from a double-mutant female mouse shows a cyst (c), hemorrhage (H), and many tubule-like structures (*arrowheads*). Several multilayered primary follicles are still present at this stage (*arrows*). G, Ovarian histology of a 22-week-old double-mutant female mouse shows multiple hemorrhagic areas (*black asterisks*) and many tubule-like structures (*white asterisks*). Very few follicles are present at the periphery (*white arrows*). Note the difference in tumor pathology compared with that seen in an inhibin-deficient female mouse ovary in panel D. H, High-power magnification of a region from the same ovary as in panel G, showing one abnormal follicle with two oocytes (*black arrows*), remnants of zona pellucida (*white arrow*), a normal follicle (*white arrowhead*), and a tubule-like structure (*black arrowhead*). At 33 weeks, only 10% of the double-mutant female mice survive and develop hemorrhagic ovarian tumors. At this stage no normal follicles are present (I). The ovarian tumor consists of aggressively proliferating cells (*asterisk*) and multiple hemorrhagic spots (*arrows*). Histological analysis of the liver from this double-mutant female mouse revealed normal liver architecture (data not shown).

to 14–16 months of age were fertile when mated to wild-type females and produced viable double-heterozygous mutant mice. The epididymal sperm number in these mice was comparable to that in age-matched control wild-type mice (data not shown). Together, these results confirm that absence of FSH leads to important functional alterations in gonadal tumors that develop in inhibin-deficient mice.

Table 2. Characteristics of Gonadal Tumors in inha^{m1}/inha^{m1}; fshb^{m1}/fshb^{m1} Double-Homozygous Mutant Mice

Mouse	Age (weeks)	Morphology and Histopathology of the Gonads	Cachexia
Males			
1–5	6–9	Normal testes, histology normal	No
6	10	Necrotic testes, hemorrhagic, seminal vesicles atrophied	No
7, 8	12	Small focal hemorrhages in both testes, initiation of tumor cell proliferation	No
9	15	Bilateral testicular tumors, hemorrhagic	No
10, 11	20	Fertile up to 12 weeks; unilateral hemorrhagic testicular tumor; only a focal tumor; resembles morphologically and histologically ovarian tumor	No
12, 13	32–34	Large distended testis, unilateral hemorrhagic tumor, infertile, enlarged urinary bladder	No
14–17	46–56	Bilateral hemorrhagic tumor, bilateral infarcted testes, one large and the other small; normal liver	No
18–20	63–67	Normal testes, no signs of aggressive tumor or hemorrhage, fertile, produced several litters of double heterozygous progeny when mated to wild-type females; very fine focal hemorrhage in one testis, other looks normal	No
Females			
1–3	6–7	Small ovaries, bilateral, hemorrhagic tumors; focal Sertoli cell tumors	No
4–6	9	Small ovaries, enlarged and thick uterus; Sertoli cell tumors; unilateral cyst	No
7	10	Small, bilateral tumors	Yes
8, 9	12	Unilateral tumor, bilateral cysts, Sertoli tubules evident	No
10, 11	18–19	Bilateral, hemorrhagic tumors; liver is normal	Yes
12–20	20–36	Large, unilateral or bilateral tumors, multinodular; liver is normal	Yes (3/9) Mild (2/9) No (4/9)

Table 3. Serum Levels of Total Activin A[a] and Estradiol[b] in inha^{m1}/inha^{m1} and inha^{m1}/inha^{m1}, fshb^{m1}/fshb^{m1} Mice

Genotype	Male		Female	
	Activin A (ng/ml)	E_2 (pg/ml)	Activin A (ng/ml)	E_2 (pg/ml)
inha^{m1}/inha^{m1}	129.9 ± 15.1[c]	148.9 ± 30.5	157.5 ± 23.5[c]	89.4 ± 23.1
inha^{m1}/inha^{m1}; fshb^{m1}/fshb^{m1}	<0.078	5.4 ± 1.5	<0.078	12.1 ± 4.9

Adult mice of 8 to >10 weeks were used, values are mean ± SEM, n = 7–16.
[a] Estimated by a human activin A enzyme-linked immunosorbent assay, sensitivity = 78 pg/ml.
[b] Estimated by an ultrasensitive liquid phase double-antibody RIA, sensitivity = 5 pg/ml.
[c] Combined average of values reported previously (10) and present study.

DISCUSSION

Rationale for Design and Generation of Gain-of-Function Transgenic Mice That Overexpress hFSH

We have targeted hFSH ectopically to multiple tissues using the well characterized mMT-1 promoter (16). This strategy resulted in production of very high basal levels of hFSH in serum, the values of which far exceed those detected in postmenopausal women. Because the biologically active gonadotropins including FSH are heterodimers, we generated independent lines of transgenic mice that harbored either a human common glycoprotein hormone α-subunit minigene or the hormone-specific hFSHβ subunit gene and then intercrossed these mice to obtain hFSH-expressing mice. Although the mMT-1 promoter is active in pituitary as confirmed by a RT-PCR performed on total RNA from MT-hFSHβ mouse pituitaries (data not shown), we have confirmed the lack of expression of hFSHβ protein in pituitary gonadotropes in these mice by a simultaneous double-immunofluorescence technique using rat LHβ and hFSHβ-specific antibodies (data not shown). Thus, these data support our hypothesis that the infertility in the female hFSHβ (subunit) transgenic mice is caused somehow by the local accumulation of the hFSHβ subunit in the ovarian interstitium. Thus, the mMT-1-driven hFSHβ transgene was mainly ectopically expressed in sites other than the normal site of FSH synthesis (*i.e.* pituitary gonadotropes).

In vitro biochemical data have demonstrated that the hFSHβ subunit alone is not or inefficiently secreted out of the cell (17). In another assay, the free β-subunit of glycoprotein hormones has been shown to compete with the heterodimeric hormones to bind their corresponding cognate gonadal receptors and inhibit hormone signaling (18). Recently, Markkula *et al.* (19) have shown the presence and/or expression of gonadotropin subunits in the ovary; however, the significance of this expression is unknown. Although we did not detect free hFSHβ subunit in the serum of MT-hFSHβ

transgenic female mice, we noticed an accumulation of large amounts of hFSHβ polypeptide in the ovaries of these mice (where mMT-1 promoter is also active). It is not clear whether this deposition interfered in an autocrine or paracrine way with the folliculogenesis and resulted in the complete infertility of these mice. However, the MT-hFSHβ male mice were fertile, and therefore we could successfully generate the hFSH-transgenic mice and study the phenotypes of these mice.

Phenotypic Characteristics of hFSH-Overexpressing Mice

We have generated an hFSH-overexpressing mouse model to study the consequences of elevated levels of FSH on reproductive function and gonadal tumorigenesis. Our results clearly suggest that ectopic production of hFSH in large quantities does not affect testicular growth and differentiation including spermatogenesis. Male MT-FSH transgenic mice were infertile and demonstrated increased epididymal sperm number and enlarged seminal vesicles resulting from elevated testosterone levels. Our data suggest that the elevated hFSH levels, signaling possibly through LH receptors in the Leydig cells, resulted in increased testosterone output.

Female transgenic mice expressing high levels of hFSH were infertile and developed hemorrhagic and cystic ovaries. They have kidney and urinary tract abnormalities secondary to elevated testosterone, estradiol, and progesterone levels in serum. These female mice died by 13 weeks of age as a result of urinary tract obstruction and had no signs of tumors. We do not know whether ovarian tumors would have eventually developed in these mice. However, our previous studies (14) with the weak hFSH expressor mice, in which serum hFSH levels (116 mIU/ml) are comparable to those in postmenopausal women, suggest that prolonged exposure to elevated FSH levels for more than 1 yr do not directly cause ovarian tumorigenesis. Female-specific characteristics of hFSH overexpression are kidney abnormalities and enlarged bladder with hFSH deposition. Although the exact mechanism for this is not clear, one possibility could be estrogen-stimulated aberrant glycosylation of liver-derived hFSH, which may give rise to insoluble acidic forms of hFSH. The majority of male transgenic mice ($>$95%) and all the female transgenic mice overexpressing hFSH were infertile. In males, the infertility could result from a failure of the functional competence of sperm or it could be caused by aberrant seminal vesicle secretions. The infertility in female transgenic mice is caused by disruption of normal folliculogenesis and the development of cysts in the ovary. As early as 2 weeks of age we could notice distinct gross morphological differences in the ovaries between wild-type controls and female transgenic mice. The ovarian and kidney phenotypes observed in the adult female transgenic mice are similar to those seen in transgenic mice in which expression of an LH analog is targeted to the pituitary (20). The elevated levels of serum testosterone in male and estradiol in female hFSH-transgenic mice could be caused by cross-talk of hFSH in large excess with the LH receptors. This suggests that elevated levels of either of the gonadotropins (*i.e.* LH or FSH) can result in pathological defects in the urogenital system.

Two independent lines of FSH-transgenic mice that differ from our present model were developed earlier. In one strain, bovine FSH expression was targeted to the mammary gland (21), using a modified rat β-casein gene-based expression system. These mice expressed bioactive hFSH up to 60 IU/ml, vectorially in milk, but not in serum, at a much lower level compared with that in our hFSH-overexpressing transgenic mice. However, no physiological/pathological consequences of this ectopic expression in milk were reported. The second strain was developed, using 10 kb of hFSHβ gene sequences (22). This hFSHβ transgene was appropriately targeted to pituitary gonadotropes and contained the necessary GnRH and steroid-responsive elements (23, 24). Whereas there was a marginal increase in serum testosterone levels and testis weight in male transgenic mice, no differences were observed in female transgenic mice. The hFSHβ mRNA in the pituitaries of this line of mice appears to be expressed at 3- to 4-fold higher levels than the endogenous mouse FSHβ mRNA (M. J. Low, personal communication). Both male and female transgenic mice of this line were fertile with no additional abnormalities in other tissues (22).

MT-hFSH Transgenic Mice as Models of Human Reproductive Disorders

The phenotypic characteristics in our hFSH-overexpressing transgenic mice resemble, to some extent, known human reproductive disorders. The infertility of hFSH-transgenic male mice could be the result of a physical obstruction by the enlarged seminal vesicles at the junction where the vas deferens opens into the urethra, thus preventing the epididymal sperm ejaculation. However, the infertility of hFSH-transgenic male mice could be caused by a reproductive behavioral defect. Further analyses are required to confirm this. In male patients who have pituitary adenomas secreting large amounts of bioactive hFSH, no testicular phenotypes were observed (25). It is not known whether or not these men were infertile. It is relevant to note that inactivating mutations in either the FSHβ subunit (5) or the FSHR in mice (26) and men (27) do not affect male fertility.

In marked contrast to the male, the results obtained with our hFSH-overexpressing female mice more closely resemble clinical features in human patients. Cyst formation and hemorrhage are often associated with ovarian cancers in postmenopausal women who also have elevated serum hFSH levels (28). More striking similarity is seen when compared with patients who suffer from an ovarian hyperstimulation syn-

drome. These patients have high estradiol levels in serum, renal abnormalities including pyelonephritis in the kidney and oligouria, and massive hemorrhage and formation of cysts in the ovary (29). In addition, a premenopausal woman patient who had pituitary adenoma secreting high levels of bioactive hFSH has also been clinically documented (30). Her serum estradiol levels were found to be high, and the ultrasound scan revealed the presence of multiple ovarian cysts in the ovary (30). Although, hFSH levels are several fold higher in our transgenic mice compared with human patients, we believe hFSH-overexpressing mice are useful to study the molecular pathobiology of some of these clinical disorders. In addition, these mice may be useful for pharmacological testing of drugs that can block hemorrhage and cyst formation in the ovary.

Genetic Dissection of Gonadal Tumor Development in Inhibin-Deficient Mice and the Role of FSH in Gonadal Sex Cord-Stromal Tumor Development

To study the complex process of gonadal growth and differentiation, we previously generated inhibin-deficient mice using a gene-targeting strategy in embryonic stem cells. These mice develop focally invasive gonadal sex cord-stromal tumors of granulosa or Sertoli cell origin with 100% penetrance and eventually die due to a severe wasting syndrome (4). Thus, inhibin is identified as a novel secreted tumor suppressor specific to the gonads. The incidence of this type of gonadal tumor in humans is rare (4), and it is not known how or if mutations in the inhibin α-subunit gene or in the inhibin signal transduction pathway cause such cancers in humans. Similar to many types of human cancers, the gonadal tumors in inhibin-deficient mice arise as focal lesions, and not all of the granulosa or Sertoli cells of the gonads demonstrate a malignant transformation and form tumors. This indicates that other secondary event(s) are necessary for malignant growth. To identify these modifier foci/factors and to dissect out the individual components involved in the cascade of events that lead to the formation of gonadal tumors in inhibin-deficient mice, we have taken a genetic approach. We have generated mice with multiple genetic lesions by selected crosses and studied how the development/progression of gonadal sex cord-stromal tumor is affected. For example, double-homozygous mutant male mice deficient in inhibin and Müllerian-inhibiting substance demonstrate synergistic effects of these two proteins in accelerating Leydig cell neoplasia (31). Double-homozygous mutant mice that lack inhibin and an activin receptor II showed continued growth of the gonadal tumors, elevated levels of serum activin, and normal livers but no characteristic cachexia (15). Therefore, activins, secreted from the gonadal tumors and signaling through type II activin receptors, have been implicated as mediators of cachexia symptoms in inhibin-deficient mice (15). In addition, based on observations from Beamer's group (32), who reported an important role of androgens in granulosa cell tumorigenesis, we generated male mice deficient in inhibin and a functionally inactive androgen receptor. Analysis of these double-mutant mice demonstrated that androgens do not influence gonadal tumor development in inhibin-deficient male mice (33).

Contrary to what was observed in our inhibin/GnRH-deficient mouse model, double-homozygous inhibin and FSH-deficient mice developed gonadal tumors. However, there was a significant delay in the tumor development/progression compared with mice deficient in inhibin alone. Interestingly, there was little or no cachexia in these mice, and the serum activin levels as well as the estradiol levels were suppressed. This suggests that the tumors in these mice are functionally different as they lack the trophic stimulation by FSH. The gender differences in mechanism of FSH action on the gonads were reported previously (34). This is reflected in the fact that female mice that lack both inhibin and FSH did exhibit some differences compared with male mice that lack these proteins. Male mice, but not female mice, deficient in both inhibin and FSH were fertile and lived longer, and the gonadal tumors histologically appeared to be less locally invasive. Inhibin/FSH double-mutant mice demonstrate different phenotypes compared with our previously characterized double-mutant mice, which lack both inhibin and GnRH. This could be explained because absence of GnRH leads to complete suppression of both LH and FSH, whereas LH is still present in double-mutant mice that lack both inhibin and FSH. Granulosa and stromal cell tumors were also observed in a proportion of transgenic female, but not male, mice that overexpress either a bovine LHβ transgene or a bovine LHβ-CTP-analog (fused to the bovine α-glycoprotein hormone subunit) in the pituitary (20). These studies, along with our present genetic analyses, suggest that altered gonadotropin ratios (*i.e.* LH/FSH) in the serum may be important in gonadal tumorigenesis. We will generate mice deficient in inhibin and LH to further distinguish the roles of LH and FSH in gonadal tumorigenesis.

Mechanisms of cell cycle regulation by gonadotropins in gonadal cells are not clearly understood. Cyclin D2, an FSH-responsive cell cycle-regulatory gene, has been shown to be up-regulated in many human ovarian granulosa cell tumors (35), and cyclin D2-deficient female mice are infertile and display hypoplastic ovaries (36). The ovarian granulosa cells from these mutant mice do not proliferate both *in vivo* and *in vitro* in response to FSH, suggesting that the FSH signal transduction pathway is impaired. It will be interesting in the future to examine how specific cell cycle events in gonadal sex cord-stromal tumors are influenced by gonadotropins.

In conclusion, we have generated two different strains of transgenic mice: one in which hFSH expression from multiple tissues is directed by a mMT-1 promoter, and the other, a double-homozygous mutant that lacks both

inhibin and FSH. These studies provide *in vivo* evidence to suggest that FSH is not directly involved in gonadal tumor formation but significantly influences the tumor progression in inhibin-deficient mice. These and previously generated gain-of-function and loss-of-function mice are important models for studying hemorrhagic cyst formation and sex cord-stromal tumor development. In addition, these mouse models will be useful in the future in formulating and testing a generalized mechanism of gonadal growth and differentiation.

MATERIALS AND METHODS

Construction of Transgenes

A 1.8-kb mMT-I promoter was inserted upstream of the 2.4-kb hCG α-minigene (37). The same promoter was also fused to 5.2 kb of the hFSHβ (17) gene sequences. The hFSHβ sequences, which were engineered to start at -100 bp (after the *Hin*dIII site) in the 5′-flanking sequences, contain all of the hFSHβ exons and introns and 1 kb 3′-flanking hFSHβ sequences. The transgene fragments were released from the vector backbone with appropriate restriction enzyme digestions, purified, and microinjectioned into fertilized eggs to produce transgenic mice (14).

Generation of Transgenic Mice

Independent lines of mice harboring either the MT-α transgene or MT-hFSHβ transgene were separately generated by standard pronuclear injections into fertilized eggs from C57BL/6/C3H $\times$ ICR hybrid mice. Stable pedigrees of transgenic mice were obtained by crossing Southern blot-positive founder (FO) mice to control wild-type littermates. Mice expressing hFSH heterodimers were generated by crossing MT-α and MT-hFSHβ lines of mice to produce double transgene-positive mice. All animal studies were conducted in accordance with the guidelines for Care and Use of Experimental Animals.

Generation of inha^{m1}/inha^{m1}, fshb^{m1}/fshb^{m1} Double-Mutant Mice

Generation of inha^{m1}/inha^{m1} (10) and fshb^{m1}/fshb^{m1} (5) mice were as described. Initially, fshb^{m1}/fshb^{m1} male mice were bred to inha^{m1}/+ female mice to obtain inha^{m1}/+, fshb^{m1}/+ double-heterozygous mice. These mice were later intercrossed to obtain inha^{m1}/inha^{m1}, fshb^{m1}/fshb^{m1} double-homozygous mutant mice at a 1:16 frequency. In addition, inha^{m1}/+, fshb^{m1}/fshb^{m1} male mice were also bred to double-heterozygous mutant female mice to increase the frequency of generating double-homozygous mutant mice to 1:8.

Southern Blot Analysis

For genotype analysis of the offspring, Southern blot analyses were performed on tail DNA samples using ^{32}P-labeled probes as previously described (5, 10). Tail DNA samples from MT-α transgenic mice were screened with a 700-bp *Hin*dIII-*Hin*dIII probe fragment, and MT-hFSHβ mice were screened with a 450-bp *Pst*I-*Bam*HI hFSHβ 3′-UTR (hFSHβ-specific) probe. The identification of the inha^{m1} and fshb^{m1} mutant alleles in mice was as described (5, 10).

Northern Blot Analysis

Total RNA was extracted from different tissues of wild-type, MT-hFSH transgenic mice and from gonadal tumors of inha^{m1}/inha^{m1}, fshb^{m1}/fshb^{m1} mice by the TRI-Reagent method (38). RNA was denatured, separated on 1.4% agarose-formaldehyde gels, and transferred to nylon membranes. The membranes were hybridized at 63 C with hCGα, hFSHβ, activin βA, or activin βB probes, washed, and exposed to autoradiographic film as described (38). The blots were stripped and rehybridized with an 18S probe as an internal control (38).

RT-PCR

Total RNA was extracted from individual pituitaries of 10 kb hFSHβ transgene MT-hFSHβ transgenic, and wild-type adult male mice by the TRI-Reagent method (38). After isopropanol precipitation and air drying of the RNA pellet, the RNA was solubilized in 6 μl diethyl pyrocarbonate-treated water, and 2 μl of an aliquot from each sample was subjected to a RT-PCR reaction using the ONE TUBE PCR kit (Boehringer Mannheim, Indianapolis, IN) according to the manufacturer's instructions. The hFSHβ-specific 3′-UTR primers used in the reactions were: 5′-AAACACAACAATGGCTTCTT-3′ (forward), 5′-ATTCCAAAGAAGTGGATCCT-3′ (reverse). The amplified 450-bp fragment was separated on a 2% agarose gel and visualized by ethidium bromide staining.

Immunohistochemistry

Adult female wild-type or MT-hFSHβ transgenic mice were transcardially perfused with 4% paraformaldehyde in PBS (pH 7.2), and the pituitaries and ovaries were collected and postfixed overnight at 4 C in the same fixative containing 10% sucrose, embedded in OCT medium, and frozen on dry ice, and 16-μm sections were cut using a cryostat. Simultaneous dual immunofluorescence was performed according to previously published procedures (21) using a hFSHβ-specific monoclonal antibody (Medix, 1:500) and a guinea pig polyclonal antiserum to rat LHβ (NIDDK, 1:1000). The antigen-bound primary antibodies were visualized by appropriate secondary antibodies conjugated to either fluorescein isothiocyanate or rhodamine isothiocyanate dyes.

Hormone Assays

Mice were Metofane anesthetized and exsanguinated by closed cardiac puncture. Sera were collected and stored frozen at -20 C until further use. Rat FSH and LH were iodinated by iodogen and chloramine-T methods (21), respectively, and RIA was performed using NIDDK kits as described (21, 39). hFSH (holoprotein) was measured by fluoroimmunoassay using a Baxter automated fluoroimmunoassay detection system according to the manufacturer's instructions. Serum testosterone (sensitivity = 0.1 ng/ml) and progesterone (sensitivity = 0.3 ng/ml) were measured using solid-phase RIA kits, and estradiol (sensitivity = 5 pg/ml) was quantitated using an ultrasensitive liquid phase double-antibody assay kit according to the manufacturer's instructions. Serum IGF-I levels were measured using a rat IGF-I RIA kit after acid-ethanol extraction as per the instructions provided by the manufacturer. The enzyme-linked immunosorbent assay for activin A was performed according to previously published methods (40).

Evaluation of the Sperm Parameters

Epididymal sperm from adult male mice (6–7 weeks) were collected into 1 ml M-2 medium by incubating at 37 C for 20

min. The sperm number and motility were calculated using a hemocytometer at a 1:20 dilution. The viability of the sperm was determined by an eosin-Y method at 1:40 dilution as described (5).

Histological Analysis

Testes and epididymides were either formalin or Bouin's fixed overnight and rinsed several times in $LiCO_3$-saturated 70% ethanol. Seminal vesicles, kidneys, bladders, and ovaries were fixed in formalin overnight. The tissues were processed and paraffin embedded, and 4-μm sections were cut and stained with PAS/hematoxylin reagents as described (10).

Superovulation Experiment

Immature ICR strain female 24-day-old mice were injected with PMSG (5 IU ip/mouse) and 48 h later with hCG (5 IU ip/mouse) and mated with MT-hFSH-transgenic male mice as described (5). Vaginal plugs were monitored the next morning to confirm matings.

Statistical Analysis

Statistical analysis was done by Student's *t* test using a Microsoft Corp. (Redford, WA) Excel (version 6.0) software program. A P value <0.05 was considered significant.

Acknowledgments

We thank Yan Wang for helping with genotype analysis and mouse weight data, Grace Hamilton and Bliss Walker for assistance with histology of specimens, Josie Peace and Roberta Crawford for hFSH fluoroimmunoassay analysis, Anthony Lau and Kim Paes for assistance with computer graphics, Dr. Sherry Cipriano for critical review of the manuscript, and Shirley Baker for aid in manuscript preparation. The gonadotropin RIA kits were provided by the Hormone Distribution Program, NIDDK, NIH, Baltimore, Maryland.

Received February 1, 1999. Revision received March 18, 1999. Accepted March 19, 1999.

Address requests for reprints to: Martin M. Matzuk, Department of Pathology, Baylor College of Medicine, One Baylor Plaza, Houston, Texas 77030. E-mail: mmatzuk@bcm.tmc.edu.

These studies were supported in part by NIH Grants CA-60651 and HD-07495 to M.M.M.

REFERENCES

1. Bousfield GR, Perry WM, Ward DN 1994 Gonadotropins: chemistry and biosynthesis. In: Knobil E, Neill JD (eds) The Physiology of Reproduction. Raven Press, New York, pp 1749–1792
2. Leung PCK, Steele GL 1992 Intracellular signaling in the gonads. Endocr Rev 13:476–498
3. Albanese C, Colin IM, Crowley WF, Ito M, Pestell RG, Weiss J, Jameson JL 1996 The gonadotropin genes: evolution of distinct mechanisms for hormonal control. Recent Prog Horm Res 51:23–58
4. Matzuk MM, Kumar TR, Shou W, Coerver KA, Lau AL, Behringer RR, Finegold MJ 1996 Transgenic models to study the roles of inhibins and activins in reproduction, oncogenesis, and development. Recent Prog Horm Res 51:123–157
5. Kumar TR, Wang Y, Lu N, Matzuk MM 1997 Follicle stimulating hormone is required for ovarian follicle maturation but not male fertility. Nat Genet 15:201–204
6. Aittomaki K, Lucena JL, Pakarinen P, Sistonen P, Tapanainen J, Gromol J, Kaskikari R, Sankila EM, Lehvaslaiho H, Engel AR, Nieschlag E, Huhtaniemi I, de la Chapelle A 1995 Mutation in the follicle-stimulating hormone receptor gene causes hereditary hypergonadotropic ovarian failure. Cell 82:959–968
7. Matzuk MM 1995 Functional analysis of mammalian members of the transforming growth factor-β. Trends Endocrinol Metab 6:6–13
8. Vale W, Bilezikjian LM, Rivier C 1994 Reproductive and other roles of inhibins and activins. In: Knobil E, Neill JD (eds) The Physiology of Reproduction. Raven Press, New York, pp 1861–1878
9. Vale W, Hsueh A, Rivier C, Yu, J 1990 In: Sporn MB, Roberts AB (eds) Peptide Growth Factors and Their Receptors. Springer-Verlag, Berlin, vol 2:211–248
10. Matzuk MM, Finegold MJ, Su J-GJ, Hsueh AJW, Bradley A 1992 α-Inhibin is a tumour-suppressor gene with gonadal specificity in mice. Nature 360:313–319
11. Matzuk MM, Finegold MJ, Mather JP, Krummen L, Lu H, Bradley A 1994 Development of cancer cachexia-like syndrome, adrenal tumors in inhibin-deficient mice. Proc Natl Acad Sci USA 91:8817–8821
12. Greer BE, Berek JS 1991 Gynecologic Oncology: Treatment Rationale and Technique. Elsevier Publishing, New York
13. Kumar TR, Wang Y, Matzuk MM 1996 Gonadotropins are essential modifier factors for gonadal tumor development in inhibin-deficient mice. Endocrinology 137: 4210–4216
14. Kumar TR, Low MJ, Matzuk MM 1998 Genetic rescue of follicle-stimulating hormone β-deficient mice. Endocrinology 139:3289–3295
15. Coerver KA, Woodruff TK, Finegold MJ, Mather J, Bradley A, Matzuk MM 1996 Activin signaling through activin receptor type II causes the cachexia-like symptoms in inhibin-deficient mice. Mol Endocrinol 10:534–543
16. Palmiter RD, Norstadt G, Gelinas RE, Hammer RE, Brinster RL 1983 Metallothionein-human GH fusion genes stimulate growth of mice. Science 222:809–814
17. Keene JL, Matzuk MM, Otani T, Fauser BCJM, Galway AB, Hsueh AJW, Boime I 1989 Expression of biologically active human follitropin in Chinese hamster ovary cells. J Biol Chem 264:4769–4775
18. Dighe RR, Muralidhar K, Moudgal NR 1979 Ability of human chorionic gonadotropin beta-subunit to inhibit the steroidogenic response to lutropin. Biochem J 180: 573–578
19. Markkula M, Kananen K, Klemi P, Hujtaniemi I 1996 Pituitary and ovarian expression of the endogenous follicle-stimulating hormone (FSH) subunit genes and an FSH β-subunit promoter-driven herpes simplex virus thymidine kinase gene in transgenic mice; specific partial ablation of FSH-producing cells by antiherpes treatment. J Endocrinol 150:265–273
20. Risma KA, Clay CM, Nett TM, Wagner T, Yun J, Nilson JH 1995 Targeted overexpression of luteinizing hormone in transgenic mice leads to infertility, polycystic ovaries, and ovarian tumors. Proc Natl Acad Sci USA 92: 1322–1326
21. Greenberg NM, Anderson JW, Hsueh AJ, Nishimori K, Reeves, JJ, deAvila DM, Ward DN, Rosen JM 1991 Expression of biologically active heterodimeric bovine follicle-stimulating hormone in milk of transgenic mice. Proc Natl Acad Sci USA 88:8327–8331
22. Kumar TR, Fairchild-Huntress V, Low MJ 1992 Gonadotrope-specific expression of the human follicle-stimulating hormone β-subunit gene in pituitaries of transgenic mice. Mol Endocrinol 6:81–90

23. Kumar TR, Low MJ 1993 Gonadal steroid hormone regulation of human and mouse follicle stimulating hormone β-subunit expression *in vivo*. Mol Endocrinol 7:898–906
24. Kumar TR, Low MJ 1995 Hormonal regulation of human follicle-stimulating hormone-β subunit gene expression: GnRH stimulation and GnRH-independent androgen inhibition. Neuroendocrinology 61:628–637
25. Galway AB, Hsueh AJ, Daneshdoost L, Zhou MH, Pavlou SN, Snyder PJ 1990 Gonadotroph adenomas in men produce biologically active follicle-stimulating hormone. J Clin Endocrinol Metab 71:907–912
26. Dierich A, Sairam MR, Monaco L, Fimia GM, Gansmuller A, LeMeur M, Sassone-Corsi P 1998 Impairing follicle-stimulating hormone (FSH) signaling *in vivo*: targeted disruption of the FSH receptor leads to aberrant gametogenesis and hormonal imbalance. Proc Natl Acad Sci USA 95:13612–13617
27. Huhtaniemi IT, Aittomaki K 1998 Mutations of follicle-stimulating hormone and its receptor: effects on gonadal function. Eur J Endocrinol 138:473–481
28. Cochrane R, Regan L 1997 Undetected gynaecological disorders in women with renal disease. Hum Reprod 12:667–670
29. Agrawal R, Chimusoro K, Payne N, van der Spuy Z, Jacobs HS 1997 Severe ovarian hyperstimulation syndrome: serum and ascitic fluid concentrations of vascular endothelial growth factor. Curr Opin Obstet Gynecol 9:141–144
30. Djerassi A, Coutifaris C, West VA, Asa SL, Kapoor SC, Pavlou SN, Snyder PJ 1995 Gonadotroph adenoma in a premenopausal woman secreting follicle-stimulating hormone and causing ovarian hyperstimulation. J Clin Endocrinol Metab 80:591–594
31. Matzuk MM, Finegold MJ, Mishina Y, Bradley A, Behringer RR 1995 Synergistic effects of inhibins and Müllerian inhibiting substance on testicular tumorigenesis. Mol Endocrinol 9:1337–1345
32. Beamer WG, Shultz KL, Tennent BJ, Shultz LD 1993 Granulosa cell tumorigenesis in genetically hypogonadal-immunodeficient mice grafted with ovaries from tumor-susceptible donors. Cancer Res 53:3741–3746
33. Shou W, Woodruff TK, Matzuk MM 1997 Role of androgens in testicular tumor development in inhibin-deficient mice. Endocrinology 138:5000–5005
34. Muttukrishna S, Groome N, Ledger W 1997 Gonadotropic control of secretion of dimeric inhibins and activin A by human granulosa-luteal cells *in vitro*. J Assist Reprod Genet 14:566–574
35. Courjal F, Louason G, Speiser P, Katsaros D, Zeillinger R, Theillet C 1996 Cyclin gene amplification and overexpression in breast and ovarian cancers: evidence for the selection of cyclin D1 in breast and cyclin E in ovarian tumors. Int J Cancer 69:247–253
36. Sicinski P, Donaher JL, Geng Y, Parker SB, Gardner H, Park MY, Robker RL, Richards JS, McGinnis LK, Biggers JD, Eppig JJ, Bronson RT, Elledge SJ, Weinberg RA 1996 Cyclin D2 is an FSH-responsive gene involved in gonadal cell proliferation and oncogenesis. Nature 384:470–474
37. Matzuk MM, Boime I 1988 The role of the asparagine-linked oligosaccharides of the alpha subunit in the secretion and assembly of human clorionic gonadotropin. J Cell Biol 106:1049–1059
38. Dong J, Albertini DF, Nishimori K, Kumar TR, Lu N, Matzuk MM 1996 Growth differentiation factor-9 is required during early ovarian folliculogenesis. Nature 383:531–535
39. Matzuk MM, Kumar TR, Bradley A 1995 Different phenotypes for mice deficient in either activins or activin receptor type II. Nature 374:356–360
40. Muttukrishna S, Fowler PA, George L, Groome NP, Knight PG 1996 Changes in peripheral serum levels of total activin A during the human menstrual cycle and pregnancy. J Clin Endocrinol Metab 81:3328–3334